British Journal of Pharmacology

British Journal of Pharmacology (2018) **175** 3581–3593 3581

RESEARCH PAPER

Antimicrobial endotoxin-neutralizing peptides promote keratinocyte migration *via* P2X7 receptor activation and accelerate wound healing *in vivo*

Correspondence Dr Günther Weindl, Institute of Pharmacy (Pharmacology and Toxicology), Freie Universität Berlin, Königin-Luise-Str. 2+4, Berlin 14195, Germany. E-mail: guenther.weindl@fu-berlin.de

Received 4 January 2018; **Revised** 1 June 2018; **Accepted** 6 June 2018

Anja Pfalzgraff[1], Sergio Bárcena-Varela[2], Lena Heinbockel[3], Thomas Gutsmann[3], Klaus Brandenburg[3], Guillermo Martinez-de-Tejada[2] and Günther Weindl[1]

[1]Institute of Pharmacy (Pharmacology and Toxicology), Freie Universität Berlin, Berlin, Germany, [2]Department of Microbiology and Parasitology, Universidad de Navarra, Pamplona, Spain, and [3]Division of Biophysics, Research Center Borstel, Leibniz-Center for Medicine and Biosciences, Borstel, Germany

BACKGROUND AND PURPOSE

Wound healing is a complex process that is essential to provide skin homeostasis. Infection with pathogenic bacteria such as *Staphylococcus aureus* can lead to chronic wounds, which are challenging to heal. Previously, we demonstrated that the antimicrobial endotoxin-neutralizing peptide Pep19-2.5 promotes artificial wound closure in keratinocytes. Here, we investigated the mechanism of peptide-induced cell migration and if Pep19-2.5 accelerates wound closure *in vivo*.

EXPERIMENTAL APPROACH

Cell migration was examined in HaCaT keratinocytes and P2X7 receptor-overexpressing HEK293 cells using the wound healing scratch assay. The protein expression of phosphorylated ERK1/2, ATP release, calcium influx and mitochondrial ROS were analysed to characterize Pep19-2.5-mediated signalling. For *in vivo* studies, female BALB/c mice were wounded and infected with methicillin-resistant *S. aureus* (MRSA) or left non-infected and treated topically with Pep19-2.5 twice daily for 6 days.

KEY RESULTS

Specific P2X7 receptor antagonists inhibited Pep19-2.5-induced cell migration and ERK1/2 phosphorylation in keratinocytes and P2X7 receptor-transfected HEK293 cells. ATP release was not increased by Pep19-2.5; however, ATP was required for cell migration. Pep19-2.5 increased cytosolic calcium and mitochondrial ROS, which were involved in peptide-induced migration and ERK1/2 phosphorylation. In both non-infected and MRSA-infected wounds, the wound diameter was reduced already at day 2 post-wounding in the Pep19-2.5-treated groups compared to vehicle, and remained decreased until day 6.

CONCLUSIONS AND IMPLICATIONS

Our data suggest the potential application of Pep19-2.5 in the treatment of non-infected and *S. aureus*-infected wounds and provide insights into the mechanism involved in Pep19-2.5-induced wound healing.

Abbreviations

AMP, antimicrobial peptide; MRSA, methicillin-resistant *Staphylococcus aureus*; oxATP, oxidized ATP; SSTIs, skin and soft tissue infections

DOI:10.1111/bph.14425

Introduction

The skin provides a protective barrier against invading pathogens, which is maintained by a complex network of physical, chemical and immunological components (Bangert *et al.*, 2011). Disruption of the skin barrier leads to wound formation, initiating a well-orchestrated wound healing process to efficiently close the wound (Kondo and Ishida, 2010). Three stages of wound healing are described comprising the inflammatory phase with blood clot formation and immune cell invasion, the re-epithelialization phase where keratinocytes of the epidermis and fibroblasts of the dermis migrate and proliferate to close the wound and the remodelling phase with collagen synthesis and formation of a mature scar (Werner and Grose, 2003). Inadequate wound recovery can lead to the formation of chronic wounds, which are challenging to heal and frequently remain in the inflammatory stage (Frykberg and Banks, 2015).

Bacterial colonization of wounds represents a pivotal complication impairing or delaying wound healing (Demidova-Rice *et al.*, 2012). *Staphylococcus aureus* is the most common cause of nosocomial wound infections and skin and soft tissue infections (SSTIs), especially methicillin-resistant *S. aureus* (MRSA) which accounts for 50% of all SSTIs. In contrast, chronic and postoperative wounds are predominantly infected with Gram-negative bacteria such as *Pseudomonas aeruginosa*, *Enterococcus* and *Acinetobacter* species (Cardona and Wilson, 2015; Esposito *et al.*, 2016; Guillamet and Kollef, 2016). These organisms belong to the so-called ESKAPE pathogens, which represent the most recalcitrant bacteria and are resistant to almost all common antibiotics (Santajit and Indrawattana, 2016). Increasing resistance is also reported against topical antibiotics such as mupirocin and fusidic acid (Mendoza and Tyring, 2010; Guillamet and Kollef, 2016). Thus, new treatment options are urgently needed.

Endogenous antimicrobial peptides (AMPs) are upregulated in all stages of wound healing demonstrating their essential role for wound recovery. As they not only display direct antimicrobial effects but additionally show various host-directed effects in each phase of the wound healing process, they offer promise as candidates for the treatment of acute and chronic wounds (Mangoni *et al.*, 2016; Pfalzgraff *et al.*, 2018). In particular, promotion of cell migration *in vitro* and re-epithelialization *in vivo* were demonstrated to be essentially regulated by AMPs (Carretero *et al.*, 2008). Several AMPs were shown to stimulate keratinocyte migration *via* **EGF receptor** (EGFR) signalling, such as the frog skin-derived AMP esculentin-1a(1-21)NH_2 (Di Grazia *et al.*, 2015) or temporins A and B (Di Grazia *et al.*, 2014).

We previously showed that the antimicrobial endotoxin-neutralizing peptide Pep19-2.5 promotes artificial wound closure in keratinocytes *via* **P2X receptors** and subsequent metalloprotease-dependent transactivation of the EGFR (Pfalzgraff *et al.*, 2016). Additionally, we demonstrated a strong anti-inflammatory effect in skin cells against cell wall-derived inflammatory toxins of Gram-positive and Gram-negative bacteria (Pfalzgraff *et al.*, 2016; Pfalzgraff *et al.*, 2017).

To gain further insights into the mechanism of Pep19-2.5-induced cell migration, we examined the potential involvement and role of purinergic receptors and characterized signalling pathways leading to metalloprotease-mediated EGFR transactivation. Furthermore, we investigated if Pep19-2.5 is capable of accelerating wound closure *in vivo*.

Methods

Cell culture

The immortalized keratinocyte cell line HaCaT (passage 40–55) (CLS Cell Lines Service, Eppelheim, Germany) and HEK293 cells (passage 5–10) (ACC 305, DSMZ, Braunschweig, Germany) were cultured in RPMI-1640 (Sigma-Aldrich, Taufkirchen, Germany) with 11.1 mM glucose containing 2 mM L-glutamine and 10% ($v v^{-1}$) heat-inactivated FCS (Biochrom, Berlin, Germany), 100 $U \cdot mL^{-1}$ penicillin and 100 $\mu g \cdot mL^{-1}$ streptomycin (not for HEK293; all from PAA Laboratories, Pasching, Austria). HEK293-null cells (Invivogen, Toulouse, France) (passage 20–25), transfected with a pUNO control plasmid, were cultured in RPMI-1640 with 11.1 mM glucose containing 2 mM L-glutamine, 10 $\mu g \cdot mL^{-1}$ blasticidin S (Invivogen) and 10% ($v v^{-1}$) heat-inactivated FCS. Before stimulation, cells were washed with PBS (Sigma-Aldrich) and basal medium without FCS was added. The cell lines were regularly tested negative for mycoplasma contamination (Venor GeM Classic Mycoplasma PCR detection kit, Minerva Biolabs, Berlin, Germany).

Peptides

Pep19-2.5 (GCKKYRRFRWKFKGKFWFWG), also termed Aspidasept, **LL-37** amide trifluoroacetate salt and melittin (GIGAVLKVLTTGLPALISWIKRKRQQ) were purchased from Bachem (Bubendorf, Switzerland). All peptides were of a purity level of at least 95% as determined by HPLC and MS.

Cell transfection

HEK293 cells were seeded in 24-well plates and transfected after 24 h with 1 μg plasmid DNA encoding for the human **P2X7 receptor** (pUNO1-hP2RX7a, Invivogen) using lipofectamine (Thermo Scientific, Darmstadt, Germany) according to the manufacturer's instructions. Cells were grown for 24 h prior to stimulation. Transfection efficiency was monitored with quantitative RT-PCR (qPCR).

RNA isolation, cDNA synthesis and quantitative RT-PCR

Total RNA isolation, cDNA synthesis and qPCR were performed as described previously (Weindl *et al.*, 2007; Weindl *et al.*, 2011). The following primers (synthesized by TIB Molbiol, Germany) were used: *G6PD*, 5′-ATCGACCACTA CCTGGGCAA-3′ and 5′-TTCTGCATCACGTCCCGGA-3′; *hP2X7R-1*, 5′-TGTG-CCTACAGGTGCTACGCC-3′ and 5′-GCCCTTCACTCTTCGGAAACTC-3′; *SDHA*, 5′-TGGGAACAA GAGGGCATCTG-3′ and 5′-CCACCACTGCATCAAATTC ATG-3′; *YWHAZ*, 5′-AGACGGAAGGTGCTGAGAAA-3′ and 5′-GAAGCATTGGGGATCAAGAA-3′. Fold difference in gene expression was normalized to the housekeeping gene *YWHAZ*, because detailed preliminary investigations using three different housekeeping genes (*G6PD*, *SDHA*, and *YWHAZ*) indicated that this gene showed the most constant level of expression.

Cell viability

Cell viability in the presence of the inhibitors was determined by the MTT assay as described previously (Do *et al.*, 2014).

In vitro scratch assay

The scratch assay was performed with HaCaT cells and HEK293 cells as described previously (Pfalzgraff *et al.*, 2016). Cells were preincubated for 2 h with 5 $\mu g \cdot mL^{-1}$ **mitomycin C** (Tocris, Wiesbaden-Nordenstadt, Germany) to prevent cell proliferation. Pep19-2.5 was added in the absence or presence of the non-competitive P2X7 receptor antagonist **KN-62** (10 μM; Sigma-Aldrich), the irreversible P2X7R receptor antagonist oxidized ATP (oxATP; 100 μM; Sigma-Aldrich), the ATPase hexokinase (1 $U \cdot mL^{-1}$; Sigma-Aldrich), the mitochondrially targeted antioxidant MitoTEMPO (10 μM) or the intracellular calcium chelator BAPTA-AM (10 μM) (both from Biomol, Hamburg, Germany). **TGFβ1** (1 $ng \cdot mL^{-1}$, Miltenyi Biotech, Bergisch Gladbach, Germany) or growth medium served as positive control. Scratches were documented under a microscope with 10× (HaCaT cells) or 5× (P2X7 receptor-transfected HEK293 cells) magnification (Axiovert 135; Carl Zeiss, Jena, Germany) equipped with a digital SLR camera (Canon EOS 1000D; Canon Germany, Krefeld, Germany) immediately after the scratching procedure and once more when kept at 37°C and 5% CO_2 for 20–24 h. Pictures were taken exactly at the same position before and after the incubation to document artificial wound closure. The experiments were repeated two or four times, and representative pictures are shown.

Western blotting

After preincubation for 1 h with KN-62 (10 μM), MitoTEMPO (10 μM) or BAPTA-AM (10 μM) HaCaT cells were stimulated for 15 min for detection of phospho-**ERK**1/2. Subsequently, cells were lysed and prepared as described previously (Bock *et al.*, 2016). After gel electrophoresis and blotting, membranes were blocked with 5% BSA (Sigma-Aldrich) for 1 h at 37°C, membranes were incubated with anti-phospho-p44/42 MAPK (catalogue number: 4370) (ERK1/2) (Thr^{202}/Tyr^{204}) (D13.14.4E) XP rabbit mAb (1:1000) (NEB, Germany) overnight at 4°C and incubated with anti-rabbit HRP-conjugated secondary antibody (catalogue number: 7074) (NEB; 1:1000) for 1 h. Then, blots were developed with SignalFire ECL reagent (NEB) and visualized by PXi Touch gel imaging system (Syngene, UK). The membranes were stripped with Restore Western Blot Stripping Buffer (Thermo Scientific) and further reprobed with anti-p44/42 MAPK (catalogue number: 4695) (ERK1/2) (137F5) rabbit mAb (all 1:1000; NEB) to confirm comparable protein loading. Values of protein expression were quantified by densitometry and normalized to p44/42 MAPK-levels using ImageJ version 1.46r.

ATP assay

The ATP assay was performed with CellTiter-Glo 2.0 (Promega, Mannheim, Germany) according to the manufacturer's instructions; 40,000 HaCaT cells per well were seeded in a 96-well plate overnight. Cells were stimulated with increasing concentrations of Pep19-2.5 or melittin, and supernatant was collected after 30 min and transferred to a white 96-well plate (Greiner Bio-One, Frickenhausen, Germany). A total of 100 μL of CellTiter-Glo 2.0 per well was added and incubated for 10 min. Afterwards, luminescence was measured with a plate reader (FLUOstar Optima).

Calcium assay

A calcium assay was performed with the Ca^{2+}-sensitive dye Calbryte 520 (Biomol, Hamburg, Germany) following the manufacturer's instructions; 40,000 HaCaT cells per well in a 96-well plate were seeded overnight. A total of 100 μL of 10 μM Calbryte 520 and 2 mM **probenecid** (Tocris, Wiesbaden, Germany) in HHBS (final concentration 5 μM and 1 mM respectively) were added to the wells, and the cells were incubated at 37°C for 45 min. The dye loading medium was replaced with 200 μM HHBS containing 1 mM probenecid. A total of 50 μL of samples were added with a pump, and fluorescence intensity was recorded over time immediately after adding the samples in a plate reader (FLUOstar Optima, BMG Labtech, Offenburg, Germany; excitation/emission = 492/520 nm).

Mitochondrial ROS

Mitochondrial ROS release was measured with MitoSOX Red (Thermo Scientific) according to the manufacturer's instructions; 100,000 HaCaT cells per well in a 24-well plate were seeded overnight. After 30 min stimulation with Pep19-2.5 or antimycin A (Sigma), cells were washed with HBSS and loaded with 5 μM MitoSOX Red for 30 min at 37°C and 5% CO_2. Afterwards, cells were analysed by flow cytometry (CytoFLEX, Beckman Coulter, Krefeld, Germany).

Mouse wound healing model

All animal experiments were approved by the Animal Research Committee of University of Navarra (Protocol 013-17) and by 'Departamento de Salud del Gobierno de Navarra' (Approval code 2017/122402) and were carried out in specific pathogen-free female BALB/C mice, 6–7 weeks of age and weighing 20–22 g (Harlan Interfauna Iberica SA, Barcelona, Spain). Animal studies are reported in compliance with the ARRIVE guidelines (Kilkenny *et al.*, 2010; McGrath and Lilley, 2015). Mice were housed in aseptic rooms in the Animal Facility of the University of Navarra with 12 h light/dark cycles and under a constant temperature of 22°C. Access to water and food was *ad libitum*. Each cage contained five mice with sawdust as bedding that was changed daily. Mice were randomly distributed into experimental groups ($n = 5$ animals per group). Animal cages were housed in a random order on the shelves, and all measurements were done in a random order with the investigator being blinded to the treatment received by each experimental unit. After 1 week of acclimatization, mice were anaesthetized with an i.p. injection of ketamine ($100 mg \cdot kg^{-1}$; Merial S.A. Barcelona, Spain) and xylazine ($5 mg \cdot kg^{-1}$; Bayer Hispania, S.L. Barcelona, Spain) and dorsally wounded with a 5 mm biopsy punch (Stiefel Farma, Madrid, Spain). Afterwards, wounds were topically treated with 20 μL of vehicle (pyrogen-free saline), Pep19-2.5 ($400 \mu g \cdot mL^{-1}$) or LL-37 ($400 \mu g \cdot mL^{-1}$) twice per day for 6 days. Every second day pictures of the wounds were taken. On day 6 post-wounding, mice were killed by cervical dislocation. Although we used the Shrum scale of severity (Shrum *et al.*, 2014), its application was not required, since animals suffered no apparent discomfort at any time. For

the mouse model of infected wounds, mice were dorsally wounded and immediately infected with $3.5 \cdot 10^4$ CFU MRSA (ATCC 43300) in 10 μL pyrogen-free saline per wound. Afterwards, wounds were topically treated as described above. A schematic diagram of the study design is presented in Figure S1. Care and handling of the animals were in accordance with the ICH and OECD international guidelines.

Statistical analysis

Data are depicted as means ± SD. All experiments were performed at least five times independently. Statistical significance of differences was determined by two-way ANOVA (for animal experiments) or one-way ANOVA (Western blots) followed by Bonferroni's multiple comparison test and considered significant at $P < 0.05$. A *post* test was only carried out if $P < 0.05$ was achieved in ANOVA and homogeneity of variances was given. Statistical analysis was performed using GraphPad Prism 6.0 (GraphPad software, San Diego, USA). The data and statistical analysis comply with the recommendations on experimental design and analysis in pharmacology (Curtis *et al.*, 2018).

Nomenclature of targets and ligands

Key protein targets and ligands in this article are hyperlinked to corresponding entries in http://www.guidetopharmacology.org, the common portal for data from the IUPHAR/BPS Guide to PHARMACOLOGY (Harding *et al.*, 2018), and are permanently archived in the Concise Guide to PHARMACOLOGY 2017/18 (Alexander *et al.*, 2017a,b,c).

Results

P2X7 receptor is critically involved in Pep19-2.5-induced cell migration in vitro

We could previously show that purinergic receptors appear to be involved in Pep19-2.5-induced keratinocyte migration (Pfalzgraff *et al.*, 2016). Various AMPs can modulate or activate the P2X7 receptor (Elssner *et al.*, 2004; Ferrari *et al.*, 2004; Sommer *et al.*, 2012) which plays a critical role in epithelial cell migration (Minns *et al.*, 2016). To gain further insights into the role of purinergic receptors for Pep19-2.5-promoted cell migration, we therefore performed a wound scratch assay with P2X7 receptor antagonists in HaCaT keratinocytes. Comparable to primary human keratinocytes (Pfalzgraff *et al.*, 2016), we observed a concentration-dependent increase in Pep19-2.5-induced cell migration (Figure 1A). While the most effective peptide concentration 1 $\mu g \cdot mL^{-1}$ accelerated cell migration comparable to the positive control TGF-β, both the non-competitive P2X7 receptor antagonist KN-62 and the irreversible antagonist oxATP abrogated peptide-induced cell migration (Figure 1B). Additionally, Pep19-2.5-induced phosphorylation of ERK1/2 was reduced in the presence of KN-62 (Figure 1C, D). Cell viability was at least 80% for the applied concentrations of the inhibitors as determined by the MTT assay (Figure S2).

The pivotal role of the P2X7 receptor in Pep19-2.5-promoted cell migration was further confirmed in P2X7 receptor-transfected HEK293 cells. In HEK293-null cells lacking the P2X7 receptor, growth medium, which served as positive control, accelerated artificial wound closure, while Pep19-2.5 was not able to accelerate cell migration compared to the untreated control in the absence of the P2X7 receptor (Figure 1E). However, in P2X7 receptor-transfected HEK293 cells (Figure S3), Pep19-2.5 strongly induced cell migration which was suppressed in the presence of KN-62 (Figure 1F).

Pep19-2.5-induced cell migration requires ATP

Recent studies reveal an involvement of the P2X7 receptor ligand **ATP** in peptide-induced P2X7 receptor activation, as demonstrated for the bee venom AMP melittin which concentration-dependently evoked ATP release from HaCaT keratinocytes (Sommer *et al.*, 2012). Therefore, we investigated if the ATPase hexokinase is able to block Pep19-2.5-induced cell migration. In fact, hexokinase reduced Pep19-2.5-induced HaCaT cell migration (Figure 2A). However, in contrast to the positive control melittin which concentration-dependently increased ATP, Pep19-2.5 did not induce ATP release (Figure 2B).

Pep19-2.5-enhanced keratinocyte cell migration depends on intracellular calcium and mitochondrial ROS

As P2X7 receptor activation leads to calcium mobilization, we further investigated if Pep19-2.5 triggers calcium release. Pep19-2.5 increased cytosolic calcium even stronger than the positive control ATP when using a buffer containing calcium (Figure 3A), while the peptide-induced, but not the ATP-induced, increase was lower in the absence of extracellular calcium (Figure 3B). Since calcium can induce mitochondrial ROS generation (Gorlach *et al.*, 2015), we examined if Pep19-2.5 can increase mitochondrial ROS in HaCaT cells. Indeed, we observed an increase of mitochondrial ROS for Pep19-2.5 which was less pronounced compared to the ROS generator antimycin A (Figure 3C). To determine if intracellular calcium and ROS are involved in peptide-mediated EGFR transactivation, we investigated phosphorylation of ERK1/2 and observed a reduction of phosphorylated ERK1/2 when preincubating with the intracellular calcium chelator BAPTA-AM and the mitochondrially targeted antioxidant MitoTEMPO compared to the peptide alone (Figure 3D). Additionally, both inhibitors were able to block peptide-induced HaCaT cell migration (Figure 3E). The inhibitors did not decrease cell viability in the MTT assay (Figure S2).

Pep19-2.5 enhances wound closure in vivo

Since Pep19-2.5 strongly promotes keratinocyte migration *in vitro*, we hypothesized that the peptide accelerates re-epithelialization *in vivo* and therefore examined its *in vivo* wound healing properties in a mouse model of excisional wound healing. LL-37 was used as reference peptide (Carretero *et al.*, 2008). Topical treatment with Pep19-2.5 considerably enhanced the rate of wound closure compared with the vehicle-treated group (Figure 4A, B). The wound diameter of Pep19-2.5- and LL-37-treated wounds decreased after treatment, while the vehicle-treated wounds initially increased in diameter and showed clear signs of inflammation. Already at day 2 after wounding, we observed a significant difference in wound diameter between the peptide- and vehicle-treated wounds. At day 6, wound

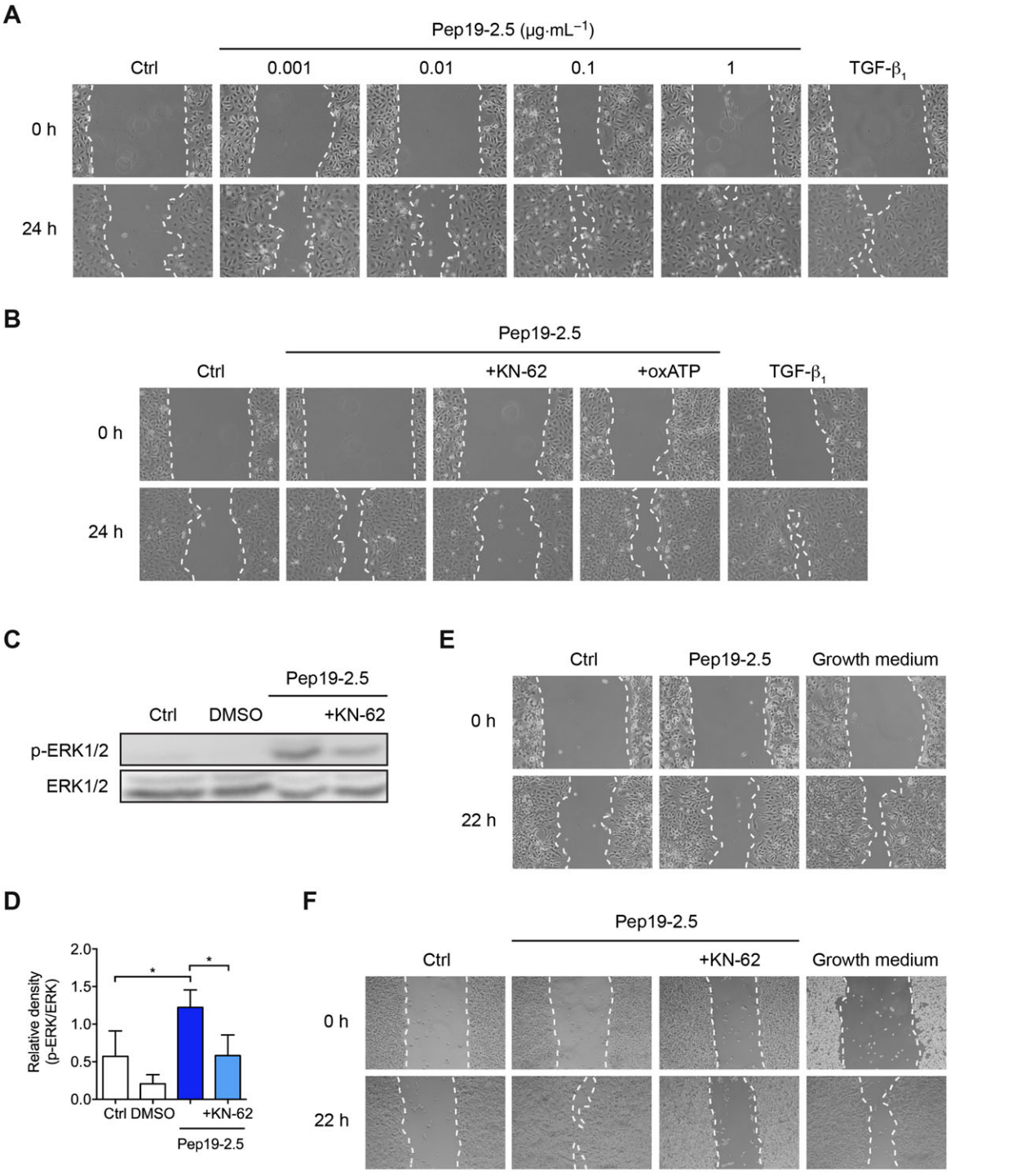

Figure 1

Peptide-induced cell migration and EGFR transactivation depends on the P2X7 receptor. (A, B) HaCaT cells were preincubated with 5 μg·mL^{-1} mitomycin C and afterwards scratched and stimulated with increasing Pep19-2.5 concentrations (A) or with 1 μg·mL^{-1} Pep19-2.5 in the presence or absence of the inhibitors KN-62 (10 μM) or oxATP (100 μM) (B). TGFβ1 served as positive control. Images were taken directly after scratching (0 h) and after 24 h and are representative of five independent experiments. (C) HaCaT cells were preincubated with KN-62 (10 μM) for 1 h and subsequently stimulated with Pep19-2.5 for 15 min. DMSO (1%, v·v^{-1}) was used as solvent control. Expression of phospho-ERK1/2 was detected by Western blot analysis. The blot is representative of five independent experiments. (D) Bar graph obtained by densitometric analysis of Western blot data. Mean + SD (n = 5). One-way ANOVA followed by Bonferroni's *post hoc* test. *$P < 0.05$. (E, F) HEK293-null cells (E) and P2X7 receptor-transfected HEK293 cells (F) were scratched and stimulated with Pep19-2.5 (1 μg·mL^{-1}) in the presence or absence of KN-62 (10 μM). Cells incubated with growth medium served as positive control. Images were taken directly after scratching (0 h) and after 22 h and are representative of five independent experiments.

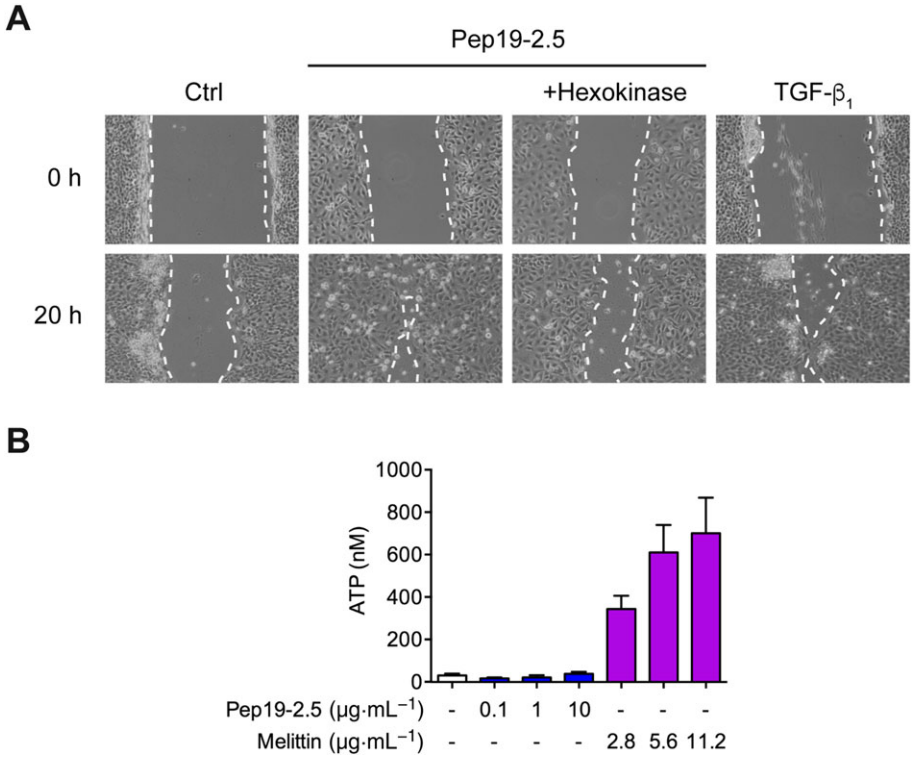

Figure 2

Role of ATP in peptide-mediated cell migration. (A) HaCaT cells were preincubated with 5 $\mu g \cdot mL^{-1}$ mitomycin C and afterwards scratched and stimulated with Pep19-2.5 in the presence or absence of the ATPase hexokinase (1 $U \cdot mL^{-1}$). TGFβ1 served as positive control. Images were taken directly after scratching (0 h) and after 20 h and are representative of five independent experiments. (B) HaCaT cells were stimulated with increasing concentrations of melittin or Pep19-2.5 for 30 min, supernatants were collected and ATP release was quantified with an ATP assay. Mean + SD (control, $n = 7$; Pep19-2.5, $n = 5$; melittin, $n = 6$).

diameters of Pep19-2.5-treated mice were reduced by 50–80%, while LL-37-treated mice showed a wound diameter reduction between 25 and 50% (Figure 4B) and the wound diameter of 2 out of 5 vehicle-treated mice was not reduced or even increased (data not shown).

Pep19-2.5 promotes closure of MRSA-infected wounds in vivo

Additionally, to inducing cell migration *in vitro*, Pep19-2.5 reduces inflammation in different skin cells stimulated with LPS and lipoproteins and neutralizes the pro-inflammatory activity of the *S. aureus* lipoprotein SitC (Martinez de Tejada *et al.*, 2015; Pfalzgraff *et al.*, 2016). Since *S. aureus* is the major cause for wound infections (Esposito *et al.*, 2016), we sought to determine the wound healing activities of Pep19-2.5 in a mouse model of MRSA skin wound infection. On day 2 post-infection, all wounds showed clear signs of inflammation such as redness and swelling (Figure 5A). The wound diameter of infected, vehicle-treated wounds increased up to day 2 and afterwards, only slowly decreased to its initial size at day 0 (Figure 5B). In contrast, Pep19-2.5- and LL-37-treated as well as non-infected, vehicle-treated wounds decreased in diameter as soon as day 2 post-treatment compared to infected, vehicle-treated control. After 6 days, wound diameters of peptide-treated mice were reduced by 25–60%.

Discussion

Impaired wound healing represents a considerable health burden affecting morbidity, mortality and health costs (Serra *et al.*, 2015). In this study, we demonstrated that the antimicrobial endotoxin-neutralizing peptide Pep19-2.5 additionally to its previously reported anti-inflammatory and cell migration-promoting activity *in vitro* accelerates wound closure *in vivo* of non-infected as well as MRSA-infected wounds in mice. Furthermore, we provide significant insights into the mechanism involved in peptide-induced cell migration suggesting a crucial role for the P2X7 receptor, intracellular calcium and ROS (Figure 6).

Endogenous AMPs play an essential role during wound recovery (Mangoni *et al.*, 2016; Pfalzgraff *et al.*, 2018). Early studies revealed that antibodies against the natural AMP LL-37 were able to inhibit re-epithelialization, while LL-37 gene transfer to excisional wounds increased re-epithelialization and granulation tissue formation in mice (Heilborn *et al.*, 2003; Carretero *et al.*, 2008). EGFR transactivation has been implicated in this mechanism, which we could recently also confirm for Pep19-2.5 (Pfalzgraff *et al.*, 2016). Transactivation of EGFR occurs *via* metalloprotease-mediated shedding of EGFR ligands that subsequently activate EGFR and downstream signalling. Furthermore, we and other groups reported that purinergic receptors play a pivotal bridging role in the peptide-

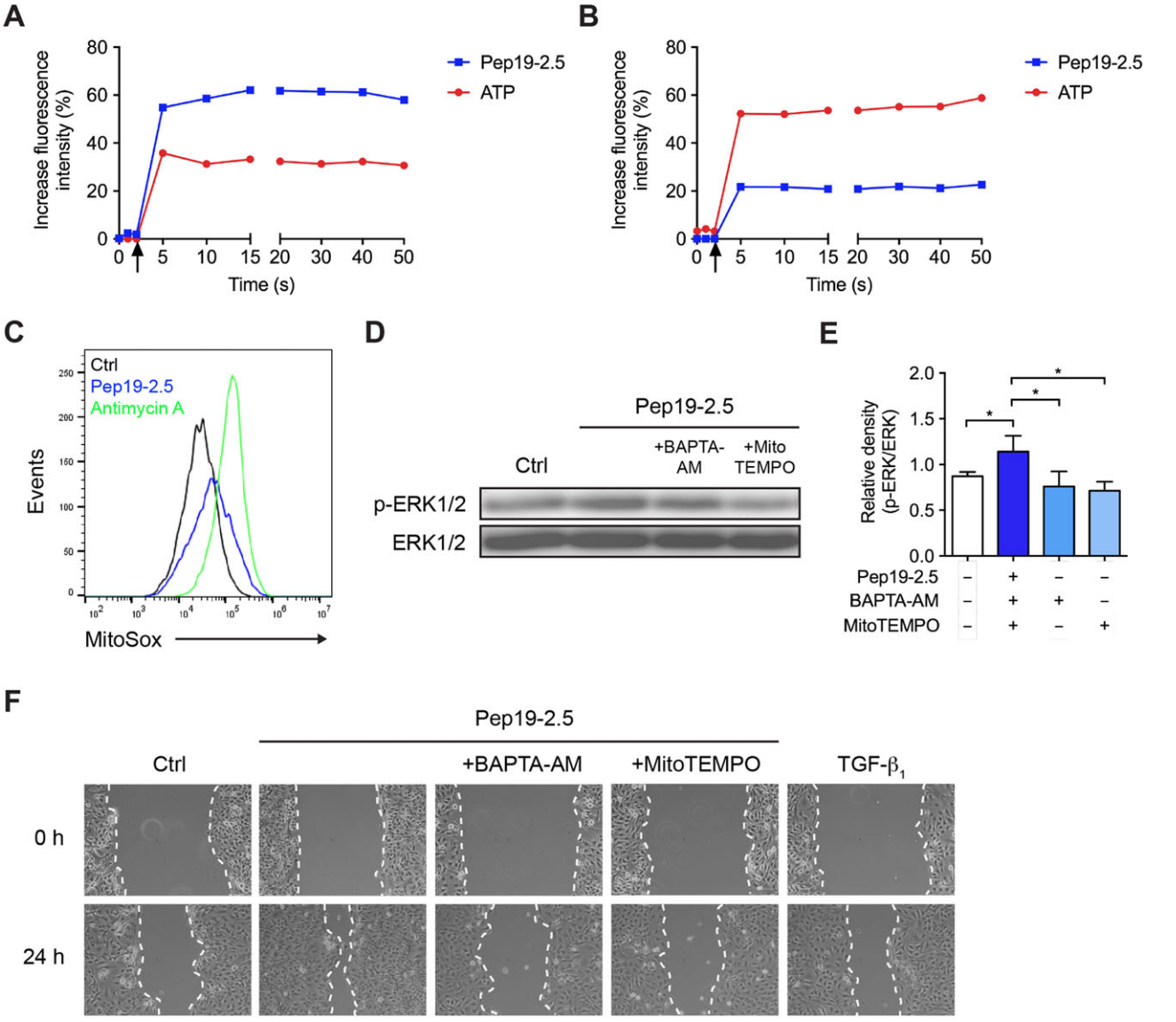

Figure 3

Calcium and ROS are involved in peptide-induced EGFR transactivation and cell migration. (A, B) HaCaT cells were loaded with Calbryte 520 and probenecid for 45 min in calcium-containing (A) or calcium-free (B) medium. Pep19-2.5 (1 $\mu g \cdot mL^{-1}$) or ATP (10 μM) was added with different pumps, and kinetic measurement of calcium release was performed immediately after addition of the samples. Arrows indicate the addition of control or stimuli. The graph is representative of five independent experiments and the results are expressed as % increase in fluorescence intensity over control. (C) HaCaT cells were stimulated with Pep19-2.5 (1 $\mu g \cdot mL^{-1}$) or antimycin A (1 μM) for 30 min and afterwards loaded with 5 μM MitoSOX Red for 30 min and analysed by flow cytometry. The histograms are representative of five independent experiments. (D) HaCaT cells were pretreated with BAPTA-AM (10 μM) or MitoTEMPO (10 μM) for 1 h and subsequently stimulated with Pep19-2.5 for 15 min. Expression of phospho-ERK1/2 was detected by Western blot analysis. The blot is representative of five independent experiments. (E) Bar graph obtained by densitometric analysis of Western blot data. Mean + SD ($n = 5$). One-way ANOVA followed by Bonferroni's *post hoc* test. *$P < 0.05$. (F) HaCaT cells were preincubated with 5 $\mu g \cdot mL^{-1}$ mitomycin C and afterwards scratched and stimulated with Pep19-2.5 in the presence or absence of the inhibitors BAPTA-AM (10 μM) or MitoTEMPO (10 μM). TGFβ1 served as positive control. Images were taken directly after scratching (0 h) and after 24 h and are representative of six independent experiments.

metalloprotease/EGFR stimulatory axis (Sommer *et al.*, 2012; Sperrhacke *et al.*, 2014). Here, we show a crucial role for the P2X7 receptor for peptide-induced phosphorylation of ERK1/2. This is in accordance with previous data for the keratinocyte-derived cationic peptide SPINK9 and melittin, the major component of bee venom, showing a decrease in peptide-induced ERK1/2 phosphorylation with P2 receptor antagonists and an increase in peptide-mediated ERK1/2 phosphorylation in P2X7 receptor-transfected HEK293 cells (Sommer *et al.*, 2012; Sperrhacke *et al.*, 2014). However, these studies did not show a direct involvement of the P2X7 receptor in peptide-induced cell migration. In contrast, we provide evidence that the P2X7 receptor is mandatory for peptide-induced keratinocyte

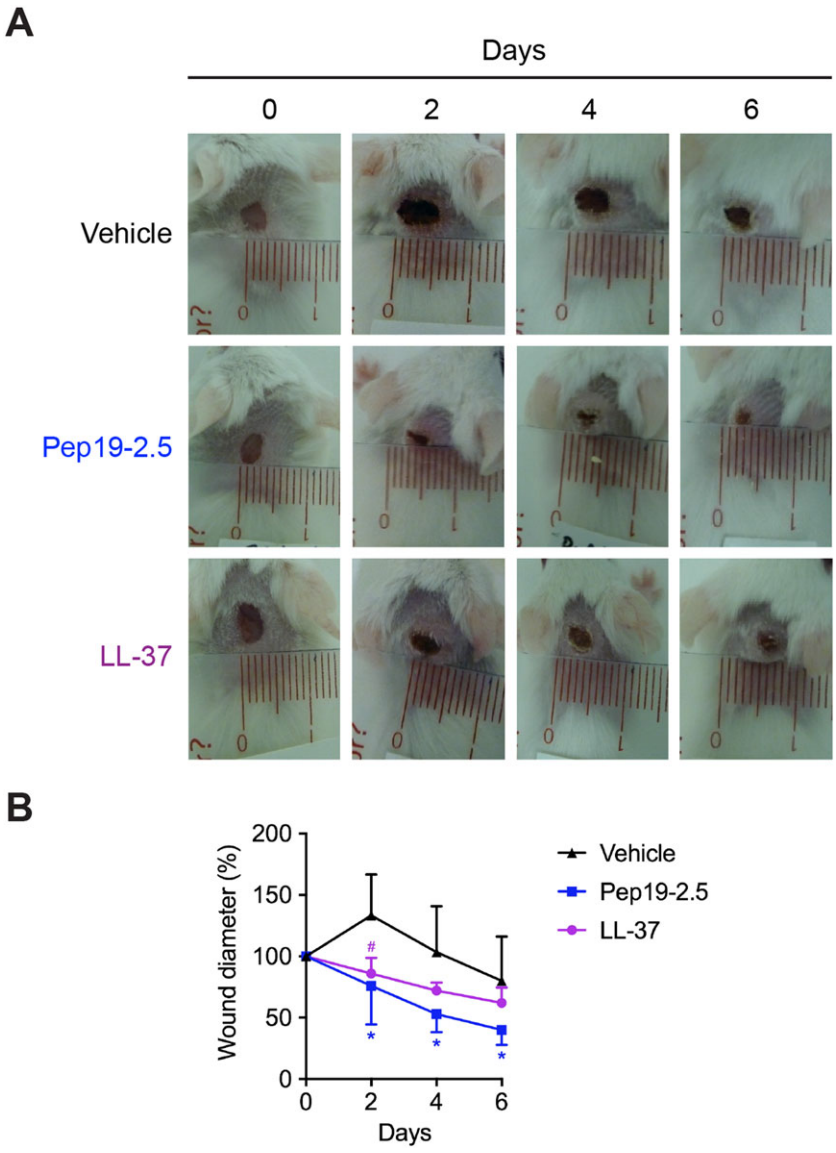

Figure 4

Pep19-2.5 accelerates wound healing *in vivo*. BALB/c mice were dorsally wounded and afterwards topically treated with vehicle (pyrogen-free saline), Pep19-2.5 (400 $\mu g \cdot mL^{-1}$) or LL-37 (400 $\mu g \cdot mL^{-1}$) twice per day for 6 days. (A) Pictures are representative for five mice per group. (B) Wound diameter for vehicle-, Pep19-2.5- and LL-37-treated wounds is depicted for day 0 to day 6. Data are mean ± SD ($n = 5$). Two-way ANOVA followed by Bonferroni's *post hoc* test. *$P < 0.05$, #$P < 0.05$. Pep19-2.5 (*) or LL-37 (#) versus vehicle-treated control.

migration which is in line with recent findings for LL-37 (Comune *et al.*, 2017). The importance of P2X7 receptor-mediated cell migration during wound healing *in vivo* remains to be established.

To get more insights into the mechanism of Pep19-2.5-mediated P2X7 receptor activation, we investigated the role of the P2X7 receptor ligand ATP. For melittin, phosphorylation of ERK1/2 in P2X7 receptor-transfected HEK cells was reduced in the presence of the ATPase apyrase indicating a critical role for ATP in melittin-induced P2X7 receptor activation. However, in HaCaT keratinocytes, the ATPase hexokinase did not completely abrogate melittin-induced ERK1/2 phosphorylation suggesting the involvement of more complex mechanisms (Sommer *et al.*, 2012). For SPINK9, ATP release was not increased and ATPases did not reduce EGFR transsignalling (Sperrhacke *et al.*, 2014). Therefore, a general role for ATP in peptide-induced P2X7 receptor activation still awaits further clarification. We could demonstrate that Pep19-2.5-induced keratinocyte migration was reduced in the presence of the ATPase hexokinase, yet Pep19-2.5 failed to increase ATP levels. We also confirmed that non-toxic concentrations of melittin increase ATP release in the nM range in HaCaT cells (Sommer *et al.*, 2012). Given the low affinity of ATP for the P2X7 receptor, concentrations in the mM range are required *in vitro* which are not commonly found in the extracellular milieu (Arulkumaran *et al.*, 2011). Therefore, we suggest that Pep19-2.5 and possibly melittin rather increase the sensitivity of the P2X7 receptor to ATP than directly

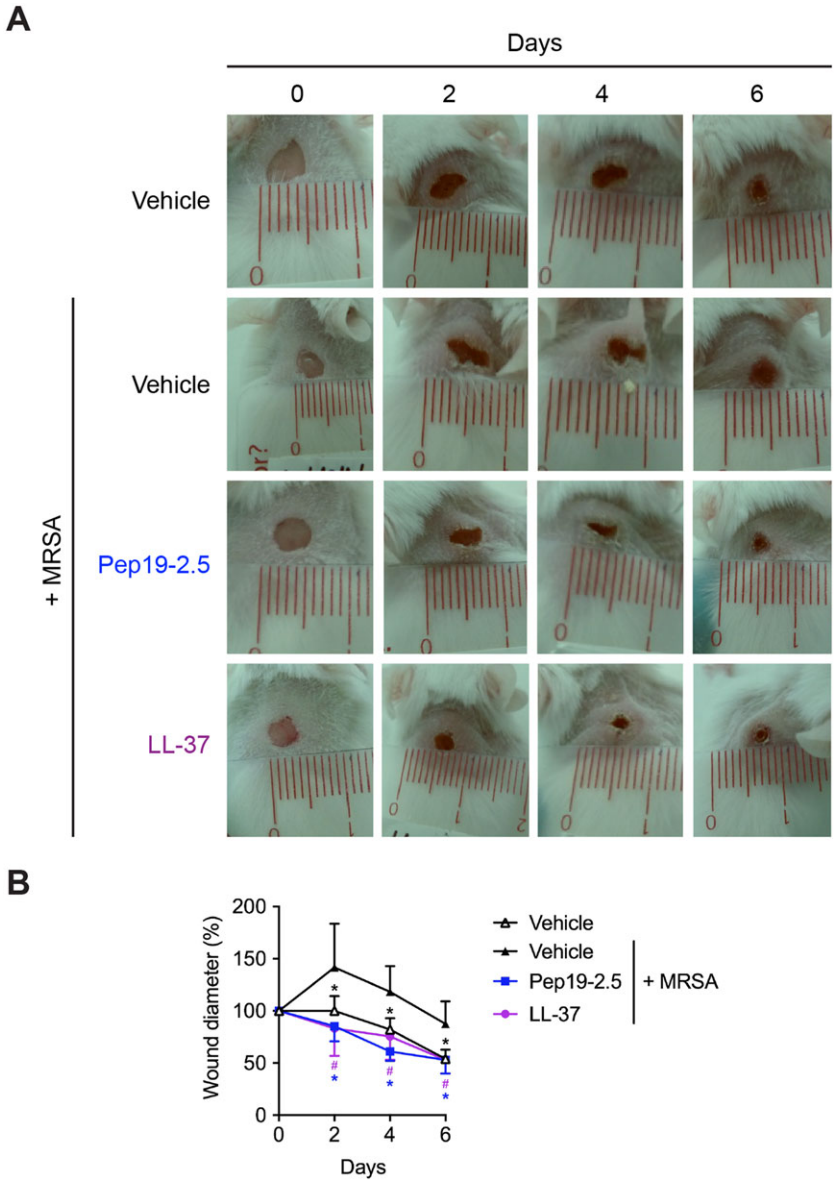

Figure 5

Pep19-2.5 promotes wound closure in MRSA-infected wounds. BALB/c mice were dorsally wounded and subsequently infected with $3.5 \cdot 10^4$ CFU MRSA in 10 μL pyrogen-free saline per wound. Afterwards, wounds were topically treated with vehicle (pyrogen-free saline) for infected or non-infected wounds, Pep19-2.5 (400 $\mu g \cdot mL^{-1}$) or LL-37 (400 $\mu g \cdot mL^{-1}$) twice per day for 6 days. (A) Pictures are representative for five mice per group. (B) Wound diameter for vehicle-, Pep19-2.5- and LL-37-treated wounds is depicted for day 0 to day 6. Data are mean ± SD (n = 5). Two-way ANOVA followed by Bonferroni's *post hoc* test. *$P < 0.05$, #$P < 0.05$. Vehicle-treated, non-infected control (*), Pep19-2.5 (*) or LL-37 (#) versus vehicle-treated, MRSA-infected control.

activating the receptor. However, it is unclear if Pep19-2.5 acts as an allosteric modulator of P2X7 receptor similar to polymyxin B (Ferrari *et al.*, 2004).

To analyse the mechanism following peptide-induced P2X7 receptor activation, we examined the capability of Pep19-2.5 to increase cytosolic calcium as P2X7 receptor activation results in increased intracellular calcium. Indeed, Pep19-2.5 induced a strong calcium release. Notably, in the absence of extracellular calcium, the calcium release induced by the peptide was decreased, but not completely abolished, compared to the release in the presence of extracellular calcium. This indicates that the observed calcium increase might be due to calcium influx from the extracellular milieu as well as release from intracellular stores as demonstrated for melittin (Tomasinsig *et al.*, 2008). Recent studies indicate that calcium influx triggered by ATP-induced P2X7 receptor activation leads to ADAM10-mediated ectodomain shedding of CD44 resulting in formation of soluble CD44 (sCD44) (Stamenkovic and Yu, 2009). Thus, the peptide-increased calcium influx could further induce sCD44-mediated allosteric activation of the P2X7 receptor through a positive feed-back loop (Moura *et al.*, 2015).

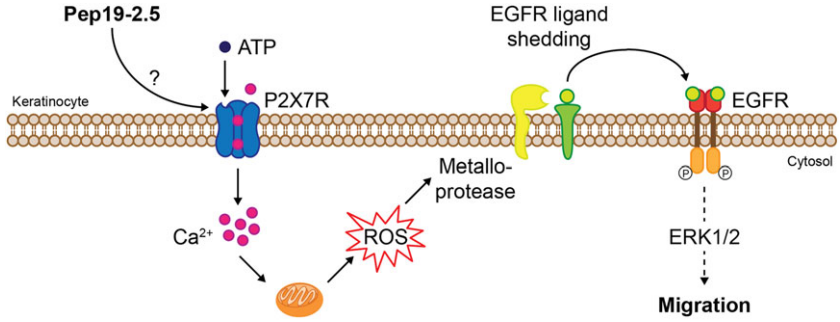

Figure 6

Proposed molecular mechanism of Pep19-2.5-induced keratinocyte migration *via* the P2X7 receptor and EGFR. Pep19-2.5 induces P2X7 receptor activation indirectly or by acting as an allosteric modulator, thus increasing its sensitivity to the extracellular ligand ATP. P2X7 receptor activation leads to Ca^{2+} mobilization, followed by mitochondrial ROS release. ROS, in turn, trigger metalloprotease-mediated EGFR transactivation resulting in downstream signalling *via* ERK1/2 and finally leading to keratinocyte migration.

As intracellular calcium is able to induce ROS formation in keratinocytes (Masaki *et al.*, 2009), we investigated the ability of Pep19-2.5 to trigger mitochondrial ROS release. Pep19-2.5-induced mitochondrial ROS release from HaCaT cells and ROS is able to activate ADAMs (Scott *et al.*, 2011). Therefore, we hypothesize that the role of the P2X7 receptor in the peptide-metalloprotease/EGFR stimulatory axis is implemented *via* intracellular calcium-induced ROS release followed by ADAM activation which in turn mediates EGFR transactivation. This is further supported by our observation that peptide-induced ERK1/2 phosphorylation and keratinocyte migration depends on calcium and ROS. Importantly, low concentrations of ROS can induce keratinocyte migration, while high concentrations can lead to chronic inflammation (Andre-Levigne *et al.*, 2017). Therefore, low amounts of ROS induced by Pep19-2.5 might be sufficient to promote cell migration without inducing cytotoxicity.

Additionally, to promotion of cell migration *in vitro*, AMPs support wound healing *in vivo* by sustaining wound re-epithelialization. The small peptide tiger 17, which promoted keratinocyte migration as well as proliferation *in vitro*, was capable of improving re-epithelialization *in vivo* (Tang *et al.*, 2014). AH90, a peptide from frog skin, accelerated wound closure *in vivo* in non-infected wounds and improved epidermal and dermal regeneration and granulation tissue formation (Liu *et al.*, 2014). Pep19-2.5 treatment resulted in rapid wound closure compared to vehicle-treated wounds as soon as day 2 post-treatment comparable to the innate defence regulator peptide IDR-1018 which also improved wound closure already at day 2 after wounding (Steinstraesser *et al.*, 2012). It remains to be determined whether Pep19.2-5 modulates other wound healing-promoting activities such as induction of angiogenesis, as recently reported for IDR-1018 (Marin-Luevano *et al.*, 2018). Considering the distinct mode of action of the aforementioned AMPs compared to Pep19-2.5, involving the release of TGF-β or immunomodulatory activities, a combination of these peptides with Pep19-2.5 might be of clinical benefit due to a possible synergistic effect.

A potential limitation of our study is that the *in vitro* findings may be less relevant *in vivo*. Wound healing in mice, but not in humans, mainly occurs *via* contraction and not re-epithelialization and granulation tissue formation (Wong *et al.*, 2011). This might explain, at least partially, the less pronounced effect of Pep19-2.5 in the mouse wound healing studies compared to the potent effect on keratinocyte migration. Thus, alternative preclinical models should be considered in future research (Ansell *et al.*, 2012).

S. aureus-secreted toxins, virulence factors and exoproteins can delay wound healing and may lead to prolonged inflammation and chronic infection. Additionally, skin infections caused by *S. aureus* or *P. aeruginosa* frequently lead to invasive infections that might result in sepsis (Thangamani *et al.*, 2015; Guillamet and Kollef, 2016). Notably, the inflammatory response after bacterial infection contributes to the clinical severity of *S. aureus* skin infection rather than the bacterial burden (Mohamed *et al.*, 2014). We could previously demonstrate a strong anti-inflammatory effect of Pep19-2.5 against pathogenicity factors of Gram-positive and Gram-negative bacteria in skin cells (Pfalzgraff *et al.*, 2016). Here, we show that Pep19-2.5 is able to accelerate wound closure in MRSA-infected wounds additionally to non-infected wounds suggesting an additional mechanism besides promoting re-epithelialization. Importantly, Pep19-2.5 shows strong activity against diverse Toll-like receptor (TLR)2 agonists found in *S. aureus* including lipopeptides such as SitC, peptidoglycans and lipoteichoic acid (Martinez de Tejada *et al.*, 2015). The relatively high MIC value of 128 $\mu g \cdot mL^{-1}$ for MRSA (Gutsmann *et al.*, 2010) suggests that Pep19-2.5, apart from the cell migration-promoting activity, improves wound healing of infected wounds due to an anti-inflammatory effect rather than a direct antimicrobial effect. This mode of action has been demonstrated for other AMPs (Thangamani *et al.*, 2015; Mohamed *et al.*, 2016) and also Pep19-2.5 which directly binds to heat-killed MRSA and reduces heat-killed MRSA-induced inflammation in *ex vivo* lung tissues (Heinbockel *et al.*, 2013).

Pep19-2.5 was designed to neutralize cell-wall derived bacterial toxins, thus acting as an anti-inflammatory agent and inhibiting TLR2 and TLR4-mediated responses. In contrast, treatment with conventional antibiotics may trigger the secretion of pro-inflammatory cytokines by releasing pathogenicity factors and therefore even worsen the outcome of an infection, as demonstrated for ciprofloxacin (Heinbockel *et al.*, 2013). By displaying activity against

pathogenicity factors of both Gram-positive and Gram-negative bacteria, Pep19-2.5 might also be used for the treatment of polymicrobial wound infections in a combination with an antibiotic to merge the anti-inflammatory and re-epithelialization promoting effect of the peptide with the direct antimicrobial effect of the antibiotic. Thus, future studies should investigate application of Pep19-2.5 in combination with antibiotics for the treatment of infected wounds. Additionally, alternative delivery methods and formulations should be considered since conjugation of LL-37 to gold nanoparticles improved *in vitro* and *in vivo* wound healing activity compared to soluble LL-37 (Comune *et al*., 2017).

In conclusion, we provide evidence for the potential application of Pep19-2.5 in the treatment of non-infected and *S. aureus*-infected wounds and give insights into the mechanism involved in Pep19-2.5-induced wound healing.

Acknowledgements

A.P. gratefully acknowledges a doctoral fellowship from the Elsa-Neumann-Scholarship program, Berlin, Germany. S.B.V. is recipient of a doctoral fellowship from Friends of the University of Navarra, Spain. G.M.T. was funded by a grant from 'Proyectos de Investigación Universidad de Navarra' (PIUNA-P2011-17), Spain. This paper contains parts of the doctoral thesis of A.P. (Pfalzgraff, 2018).

Author contributions

A.P., G.M.T. and G.W. conceived and designed the experiments. A.P. and S.B.V. conducted the experiments. L.H. and K.B. contributed essential reagents. A.P., S.B.V., G.M.T. and G.W. performed the analysis of data. A.P. and G.W. wrote the manuscript. All authors read and approved the final manuscript.

Conflict of interest

The authors declare no conflicts of interest.

Declaration of transparency and scientific rigour

This Declaration acknowledges that this paper adheres to the principles for transparent reporting and scientific rigour of preclinical research recommended by funding agencies, publishers and other organisations engaged with supporting research.

References

Alexander SPH, Fabbro D, Kelly E, Marrion NV, Peters JA, Faccenda E *et al*. (2017a). The Concise Guide to PHARMACOLOGY 2017/18: Catalytic receptors. Br J Pharmacol 174: S225–S271.

Alexander SPH, Peters JA, Kelly E, Marrion NV, Faccenda E, Harding SD *et al*. (2017b). The Concise Guide to PHARMACOLOGY 2017/18: Ligand-gated ion channels. Br J Pharmacol 174: S130–S159.

Alexander SPH, Fabbro D, Kelly E, Marrion NV, Peters JA, Faccenda E *et al*. (2017c). The Concise Guide to PHARMACOLOGY 2017/18: Enzymes. Br J Pharmacol 174: S272–S359.

Andre-Levigne D, Modarressi A, Pepper MS, Pittet-Cuenod B (2017). Reactive oxygen species and NOX enzymes are emerging as key players in cutaneous wound repair. Int J Mol Sci 18: 2149.

Ansell DM, Holden KA, Hardman MJ (2012). Animal models of wound repair: are they cutting it? Exp Dermatol 21: 581–585.

Arulkumaran N, Unwin RJ, Tam FW (2011). A potential therapeutic role for P2X7 receptor (P2X7R) antagonists in the treatment of inflammatory diseases. Expert Opin Investig Drugs 20: 897–915.

Bangert C, Brunner PM, Stingl G (2011). Immune functions of the skin. Clin Dermatol 29: 360–376.

Bock S, Pfalzgraff A, Weindl G (2016). Sphingosine 1-phospate differentially modulates maturation and function of human Langerhans-like cells. J Dermatol Sci 82: 9–17.

Cardona AF, Wilson SE (2015). Skin and soft-tissue infections: a critical review and the role of telavancin in their treatment. Clin Infect Dis 61 (Suppl 2): S69–S78.

Carretero M, Escamez MJ, Garcia M, Duarte B, Holguin A, Retamosa L *et al*. (2008). In vitro and *in vivo* wound healing-promoting activities of human cathelicidin LL-37. J Invest Dermatol 128: 223–236.

Comune M, Rai A, Chereddy KK, Pinto S, Aday S, Ferreira AF *et al*. (2017). Antimicrobial peptide-gold nanoscale therapeutic formulation with high skin regenerative potential. J Control Release 262: 58–71.

Curtis MJ, Alexander S, Cirino G, Docherty JR, George CH, Giembycz MA *et al*. (2018). Experimental design and analysis and their reporting II: updated and simplified guidance for authors and peer reviewers. Br J Pharmacol 175: 987–993.

Demidova-Rice TN, Hamblin MR, Herman IM (2012). Acute and impaired wound healing: pathophysiology and current methods for drug delivery, part 1: normal and chronic wounds: biology, causes, and approaches to care. Adv Skin Wound Care 25: 304–314.

Di Grazia A, Cappiello F, Imanishi A, Mastrofrancesco A, Picardo M, Paus R *et al*. (2015). The frog skin-derived antimicrobial peptide esculentin-1a (1-21)NH2 promotes the migration of human HaCaT keratinocytes in an EGF receptor-dependent manner: a novel promoter of human skin wound healing? PLoS One 10: e0128663.

Di Grazia A, Luca V, Segev-Zarko LA, Shai Y, Mangoni ML (2014). Temporins A and B stimulate migration of HaCaT keratinocytes and kill intracellular Staphylococcus aureus. Antimicrob Agents Chemother 58: 2520–2527.

Do N, Weindl G, Grohmann L, Salwiczek M, Koksch B, Korting HC *et al*. (2014). Cationic membrane-active peptides – anticancer and antifungal activity as well as penetration into human skin. Exp Dermatol 23: 326–331.

Elssner A, Duncan M, Gavrilin M, Wewers MD (2004). A novel P2X7 receptor activator, the human cathelicidin-derived peptide LL37, induces IL-1 beta processing and release. J Immunol 172: 4987–4994.

Esposito S, Noviello S, Leone S (2016). Epidemiology and microbiology of skin and soft tissue infections. Curr Opin Infect Dis 29: 109–115.

Ferrari D, Pizzirani C, Adinolfi E, Forchap S, Sitta B, Turchet L *et al*. (2004). The antibiotic polymyxin B modulates P2X7 receptor function. J Immunol 173: 4652–4660.

Frykberg RG, Banks J (2015). Challenges in the treatment of chronic wounds. Adv Wound Care (New Rochelle) 4: 560–582.

Gorlach A, Bertram K, Hudecova S, Krizanova O (2015). Calcium and ROS: a mutual interplay. Redox Biol 6: 260–271.

Guillamet CV, Kollef MH (2016). How to stratify patients at risk for resistant bugs in skin and soft tissue infections? Curr Opin Infect Dis 29: 116–123.

Gutsmann T, Razquin-Olazaran I, Kowalski I, Kaconis Y, Howe J, Bartels R *et al*. (2010). New antiseptic peptides to protect against endotoxin-mediated shock. Antimicrob Agents Chemother 54: 3817–3824.

Harding SD, Sharman JL, Faccenda E, Southan C, Pawson AJ, Ireland S *et al*. (2018). The IUPHAR/BPS Guide to PHARMACOLOGY in 2018: updates and expansion to encompass the new guide to IMMUNOPHARMACOLOGY. Nucl Acids Res 46: D1091–D1106.

Heilborn JD, Nilsson MF, Kratz G, Weber G, Sorensen O, Borregaard N *et al*. (2003). The cathelicidin anti-microbial peptide LL-37 is involved in re-epithelialization of human skin wounds and is lacking in chronic ulcer epithelium. J Invest Dermatol 120: 379–389.

Heinbockel L, Sanchez-Gomez S, Martinez de Tejada G, Domming S, Brandenburg J, Kaconis Y*et al*. (2013). Preclinical investigations reveal the broad-spectrum neutralizing activity of peptide Pep19-2.5 on bacterial pathogenicity factors. Antimicrob Agents Chemother 57: 1480–1487.

Kilkenny C, Browne W, Cuthill IC, Emerson M, Altman DG (2010). Animal research: reporting *in vivo* experiments: the ARRIVE guidelines. Br J Pharmacol 160: 1577–1579.

Kondo T, Ishida Y (2010). Molecular pathology of wound healing. Forensic Sci Int 203: 93–98.

Liu H, Mu L, Tang J, Shen C, Gao C, Rong M *et al*. (2014). A potential wound healing-promoting peptide from frog skin. Int J Biochem Cell Biol 49: 32–41.

Mangoni ML, McDermott AM, Zasloff M (2016). Antimicrobial peptides and wound healing: biological and therapeutic considerations. Exp Dermatol 25: 167–173.

Marin-Luevano P, Trujillo V, Rodriguez-Carlos A, Gonzalez-Curiel I, Enciso-Moreno JA, Hancock REW*et al*. (2018). Induction by innate defence regulator peptide 1018 of pro-angiogenic molecules and endothelial cell migration in a high glucose environment. Peptides 101: 135–144.

Martinez de Tejada G, Heinbockel L, Ferrer-Espada R, Heine H, Alexander C, Barcena-Varela S *et al*. (2015). Lipoproteins/peptides are sepsis-inducing toxins from bacteria that can be neutralized by synthetic anti-endotoxin peptides. Sci Rep 5: 14292.

Masaki H, Izutsu Y, Yahagi S, Okano Y (2009). Reactive oxygen species in HaCaT keratinocytes after UVB irradiation are triggered by intracellular Ca (2+) levels. J Investig Dermatol Symp Proc 14: 50–52.

McGrath JC, Lilley E (2015). Implementing guidelines on reporting research using animals (ARRIVE etc.): new requirements for publication in BJP. Br J Pharmacol 172: 3189–3193.

Mendoza N, Tyring SK (2010). Emerging drugs for complicated skin and skin-structure infections. Expert Opin Emerg Drugs 15: 509–520.

Minns MS, Teicher G, Rich CB, Trinkaus-Randall V (2016). Purinoreceptor P2X7 regulation of Ca (2+) mobilization and cytoskeletal rearrangement is required for corneal reepithelialization after injury. Am J Pathol 186: 285–296.

Mohamed MF, Abdelkhalek A, Seleem MN (2016). Evaluation of short synthetic antimicrobial peptides for treatment of drug-resistant and intracellular Staphylococcus aureus. Sci Rep 6: 29707.

Mohamed MF, Hamed MI, Panitch A, Seleem MN (2014). Targeting methicillin-resistant Staphylococcus aureus with short salt-resistant synthetic peptides. Antimicrob Agents Chemother 58: 4113–4122.

Moura G, Lucena SV, Lima MA, Nascimento FD, Gesteira TF, Nader HB *et al*. (2015). Post-translational allosteric activation of the P2X7 receptor through glycosaminoglycan chains of CD44 proteoglycans. Cell Death Discovery 1: 15005.

Pfalzgraff A (2018). Investigations on the activity of synthetic anti-lipopolysaccharide peptides against cytoplasmic lipopolysaccharide-induced responses and their anti-inflammatory and wound healing-promoting effect in the skin (Doctoral dissertation). Retrieved from Refubium - Freie Universität Berlin Repository. (Accession No. 000000107221).

Pfalzgraff A, Brandenburg K, Weindl G (2018). Antimicrobial peptides and their therapeutic potential for bacterial skin infections and wounds. Front Pharmacol 9: 281.

Pfalzgraff A, Heinbockel L, Su Q, Brandenburg K, Weindl G (2017). Synthetic anti-endotoxin peptides inhibit cytoplasmic LPS-mediated responses. Biochem Pharmacol 140: 64–72.

Pfalzgraff A, Heinbockel L, Su Q, Gutsmann T, Brandenburg K, Weindl G (2016). Synthetic antimicrobial and LPS-neutralising peptides suppress inflammatory and immune responses in skin cells and promote keratinocyte migration. Sci Rep 6: 31577.

Santajit S, Indrawattana N (2016). Mechanisms of antimicrobial resistance in ESKAPE pathogens. Biomed Res Int 2016: 2475067.

Scott AJ, O'Dea KP, O'Callaghan D, Williams L, Dokpesi JO, Tatton L *et al*. (2011). Reactive oxygen species and p38 mitogen-activated protein kinase mediate tumor necrosis factor alpha-converting enzyme (TACE/ADAM-17) activation in primary human monocytes. J Biol Chem 286: 35466–35476.

Serra R, Grande R, Butrico L, Rossi A, Settimio UF, Caroleo B *et al*. (2015). Chronic wound infections: the role of Pseudomonas aeruginosa and Staphylococcus aureus. Expert Rev Anti Infect Ther 13: 605–613.

Shrum B, Anantha RV, Xu SX, Donnelly M, Haeryfar SM, McCormick JK *et al*. (2014). A robust scoring system to evaluate sepsis severity in an animal model. BMC Res Notes 7: 233.

Sommer A, Fries A, Cornelsen I, Speck N, Koch-Nolte F, Gimpl G *et al*. (2012). Melittin modulates keratinocyte function through P2 receptor-dependent ADAM activation. J Biol Chem 287: 23678–23689.

Sperrhacke M, Fischer J, Wu Z, Klunder S, Sedlacek R, Schroeder JM *et al*. (2014). SPINK9 stimulates metalloprotease/EGFR-dependent keratinocyte migration via purinergic receptor activation. J Invest Dermatol 134: 1645–1654.

Stamenkovic I, Yu Q (2009). Shedding light on proteolytic cleavage of CD44: the responsible sheddase and functional significance of shedding. J Invest Dermatol 129: 1321–1324.

Steinstraesser L, Hirsch T, Schulte M, Kueckelhaus M, Jacobsen F, Mersch EA *et al*. (2012). Innate defense regulator peptide 1018 in wound healing and wound infection. PLoS One 7: e39373.

Tang J, Liu H, Gao C, Mu L, Yang S, Rong M *et al*. (2014). A small peptide with potential ability to promote wound healing. PLoS One 9: e92082.

Thangamani S, Nepal M, Chmielewski J, Seleem MN (2015). Antibacterial activity and therapeutic efficacy of Fl-P (R) P (R) P (L)-5, a cationic amphiphilic polyproline helix, in a mouse model of staphylococcal skin infection. Drug Des Devel Ther 9: 5749–5754.

Tomasinsig L, Pizzirani C, Skerlavaj B, Pellegatti P, Gulinelli S, Tossi A *et al*. (2008). The human cathelicidin LL-37 modulates the activities of the P2X7 receptor in a structure-dependent manner. J Biol Chem 283: 30471–30481.

Weindl G, Castello F, Schäfer-Korting M (2011). Evaluation of anti-inflammatory and atrophogenic effects of glucocorticoids on reconstructed human skin. Altern Lab Anim 39: 173–187.

Weindl G, Naglik JR, Kaesler S, Biedermann T, Hube B, Korting HC *et al*. (2007). Human epithelial cells establish direct antifungal defense through TLR4-mediated signaling. J Clin Invest 117: 3664–3672.

Werner S, Grose R (2003). Regulation of wound healing by growth factors and cytokines. Physiol Rev 83: 835–870.

Wong VW, Sorkin M, Glotzbach JP, Longaker MT, Gurtner GC (2011). Surgical approaches to create murine models of human wound healing. J Biomed Biotechnol 2011: 969618.

Supporting Information

Additional supporting information may be found online in the Supporting Information section at the end of the article.

https://doi.org/10.1111/bph.14425

Figure S1 Experimental setup for *in vivo* wound healing experiments.
Figure S2 HaCaT cells were stimulated for 24 h with inhibitors and cell viability was analysed by MTT assay. DMSO (0.2, 1 and 5%, v/v) served as controls. Data are mean + SD (n = 6).
Figure S3 HEK293 cells were transfected with 0.1 μg pUNO1 plasmid encoding for human P2X7 receptor using lipofectamine. After 24 h, gene expression of *hP2X7R* was determined by qPCR. mRNA expression values were normalised to *YWHAZ*. Data are mean + SD (n = 5).